Title

Hybrid Feedback for Global Asymptotic Stabilization on a Compact Manifold

ISBN

9781509028733

Authors

Casau, Pedro
Cunha, Rita
Sanfelice, Ricardo G
et al.

Publication Date

2017-12-01

DOI

10.1109/cdc.2017.8263998

Peer reviewed

Hybrid Feedback for Global Asymptotic Stabilization on a Compact Manifold

Pedro Casau, Rita Cunha, Ricardo G. Sanfelice, Carlos Silvestre

***Abstract*— In this paper, we employ a hybrid feedback control strategy to globally asymptotically stabilize a setpoint on a smooth compact manifold without boundary satisfying the following: there exists a finite maximal atlas such that the desired setpoint belongs to each chart of the atlas. The proposed hybrid controller includes a proportional-derivative (PD) action during flows and, at jumps, uses hysteresis to switch between local coordinate charts to stabilize the desired setpoint robustly with respect to exogenous disturbances. We show that the proposed controller can be used for attitude stabilization of a rigid body and we illustrate the behavior of the closed-loop system via simulation results.**

I. Introduction

A dynamical system is usually comprised of a state-space – the set of points where the system state lies – and of ordinary differential equations, whose solutions determine the evolution of the state as a function of time. The analysis of the stability of a setpoint on the state space dates back to [1] and, depending on the nature of the system, one may resort to analysis tools for systems evolving on the n-dimensional Euclidean space (see e.g. [2]) or geometric analysis of dynamical systems if the system evolves on a more general manifold (see e.g. [3], [4] and [5]).

For the case of dynamical systems with inputs, one is interested in designing controllers such that the behaviour of the closed-loop system follows a desired pattern. This task has seen many successes in the scope of linear dynamical systems, where it was shown that controllability equates to the existence of optimal feedback laws. For the case of nonlinear systems, however, it has been shown in [6] that continuous state-feedback laws fail to provide global asymptotic stability of a setpoint for dynamical systems evolving on compact manifolds. To address this problem, alternative strategies based on nonsmooth feedback laws have been developed: for instance, in [7], a sample-and-hold stabilization strategy is proposed to globally s-stabilize a given set and, in [8] a nonsmooth control law is proposed to globally asymptotically stabilize a reference in the unit-quaternion group. However, it has been shown in [9] that, if a set cannot be globally asymptotically stabilized by means of a continuous state-feedback law, then it cannot be robustly globally asymptotically stabilized by a discontinuous state-feedback law either. A particular control synthesis tool that emerged to address the topological obstructions to global asymptotic stabilization on compact manifolds is known as synergistic hybrid feedback (see e.g. [10], [11], [12] and references therein).

Synergistic hybrid feedback is a hybrid control strategy whose popularity has been increasing over the past few years. This control strategy draws its name from the quintessential ingredient that composes it: synergistic potential functions. These are collections of functions with the following property: for each unstable equilibrium point of the gradient vector field of a given function, there exists another function in the family that has a lower value. By monitoring the difference between the value of the function currently used and the lowest possible value among all functions in the collection, it is possible to globally asymptotically stabilize a given reference by switching between gradient-based vector fields whenever a given amount is exceeded.

The first hybrid controllers for synergistic hybrid feedback were presented in [13], but it was not until [10] that synergistic potential functions became to be known by this name. This novel hybrid control technique spawned a plethora of contributions on global asymptotic stabilization on compact manifolds, including, most notably, the two-dimensional sphere [14], the three-dimensional sphere [15] and the special orthogonal group [16], [17]. It has also found applications in attitude stabilization [18], rigid-body vehicle stabilization and tracking [19], tracking for quadrotor vehicles and navigation, thus constituting a notable advancement for the problem of stabilization on compact manifolds [6] and ensuing problems [20].

In this paper, we draw inspiration from existing synergistic hybrid feedback strategies to develop a hybrid controller that globally asymptotically stabilizes a given setpoint on a compact smooth manifold without boundary. To represent the

P. Casau is with the Department of Electrical and Computer Engineering, Faculty of Science and Technology, University of Macau, Taipa, Macau, and also with the Institute for Systems and Robotics, Instituto Superior Técnico, Universidade de Lisboa, 1049-001 Lisbon, Portugal. Email: pcasau@isr.ist.utl.pt.

Rita Cunha is with Institute for Systems and Robotics, Instituto Superior Técnico, Universidade de Lisboa, Portugal. Email: rita@isr.tecnico.ulisboa.pt.

R. G. Sanfelice is with the Department of Computer Engineering, University of California, Santa Cruz, CA 95064, USA. Email: ricardo@ucsc.edu.

C. Silvestre is with the Department of Electrical and Computer Engineering, Faculty of Science and Technology, University of Macau, Taipa, Macau, on leave from Instituto Superior Técnico, Universidade de Lisboa, 1049-001 Lisbon, Portugal. Email: csilvestre@umac.mo.

This work was supported by the Macao Science and Technology Development Fund under Grants FDCT/048/2014/A1 and FDCT/026/2017/A1, by the University of Macau, Macao, China, under Projects MYRG2015-00127-FST and MYRG2016-00097-FST, by the Fundação para a Ciência e a Tecnologia (FCT) through ISR under LARSyS FCT [UID/EEA/50009/2013], project PTDC/EEI-AUT/5048/2014, the FCT Investigator Programme IF/00921/2013, and by the Ph.D. Student Scholarship SFRH/BD/70656/2010. Research by R. G. Sanfelice was partially supported by the National Science Foundation under CAREER Grant no. ECS-1450484 and Grant no. CNS-1544396, and by the Air Force Office of Scientific Research under Grant no. FA9550-16-1-0015.

dynamical system, we make use of a embedding on a higher dimensional Euclidean space, while the proposed controller employs a proportional-derivative (PD) control law which implements negative feedback of local coordinates (charts) in order to steer the system towards the desired setpoint, under the assumption that the setpoint belongs to each chart in the atlas that defines the manifold. This approach is general and, unlike earlier contributions which focused on a particular manifold of interest, such as the unit-quaternion group [15], the special orthogonal group [16] or the n-dimensional sphere [21], the proposed controller is not tied to a particular manifold. A second benefit of the proposed approach with respect to synergistic hybrid feedback is that the so-called synergy gap, which regulates controller switching, can be set arbitrarily high, thus endowing the system with additional robustness to exogenous perturbations. Also, solutions to the closed-loop system are endowed with nominal robustness to measurement noise because the system satisfies some regularity conditions, known as the hybrid basic conditions (c.f. [22, Assumption 6.5]). Finally, we illustrate these key points with the application of the proposed controller to the global asymptotic stabilization of the attitude of the rigid-body and ensuing simulation results.

This paper is organized as follows. In Section II, we present some notation and definitions that are used throughout the paper. In Section III, we describe precisely the stabilization problem. In Section IV, we present the controller design. In Section V, we present the simulation results and in Section VI, we end the paper with some concluding remarks.

II. Preliminaries & Notation

The symbols $\mathbb{R}$ and $\mathbb{N}$ represent the set of real numbers and nonnegative integers, respectively. The n-dimensional Euclidean space is represented by $\mathbb{R}^n$ and it is equipped with the inner product $\langle u, v\rangle := u^\top v$ for each $u, v \in \mathbb{R}^n$ and the norm $|x| := \sqrt{\langle x, x\rangle}$ for each $x \in \mathbb{R}^n$. The symbol e_i^n represents a vector in $\mathbb{R}^n$ whose components are zero, except for the i-th component, which is equal to 1 (we drop the superscript, whenever the dimension of the vector can be inferred from the context). The set of $m \times n$ matrices is denoted by $\mathbb{R}^{m\times n}$ and the Kronecker product between two matrices A and B is denoted by $A \otimes B$. The $n \times n$ identity matrix is denoted by I_n. The operator $\mathrm{vec} : \mathbb{R}^{m\times n} \to \mathbb{R}^{mn}$ is given by $\mathrm{vec}(A) := \begin{bmatrix}(Ae_1)^\top & \dots & (Ae_n)^\top\end{bmatrix}^\top$ for each $A \in \mathbb{R}^{m\times n}$ and $\mathsf{M}_{m,n} : \mathbb{R}^{mn} \to \mathbb{R}^{m\times n}$ denotes its inverse. The trace of a matrix $A \in \mathbb{R}^{n\times n}$ is denoted by $\mathrm{tr}(A)$.

Given a function $\psi : \mathcal{M} \to \mathcal{N}$, the image of a set $U \subset \mathcal{M}$ through ψ is given by $\psi(U) := \{y \in \mathcal{N} : y = \psi(x) \text{ for some } x \in U\}$, and the inverse image of a set $V \subset \mathcal{N}$ is given by $\psi^{-1}(V) := \{x \in \mathcal{M} : \psi(x) \in V\}$. If ψ is invertible, then ψ^{-1} denotes the inverse of ψ.

The derivative of a differentiable matrix function with matrix arguments $F : \mathbb{R}^{m\times n} \to \mathbb{R}^{k\times \ell}$ is given by

$$\mathcal{D}F(X) := \frac{\partial\, \mathrm{vec}(F(X))}{\partial\, \mathrm{vec}(X)^\top}$$

for each $X \in \mathbb{R}^{m\times n}$. For scalar functions with vector arguments $V : \mathbb{R}^n \to \mathbb{R}$, we make use of the alternative notation $\nabla V(x) := \mathcal{D}V(x)$, for each $x := (x_1, \dots, x_n) \in \mathbb{R}^n$.

A hybrid system $\mathcal{H}$ with state space $\mathbb{R}^n$ is defined as follows:

$$\begin{aligned}\dot\xi &\in F(\xi) \quad \xi \in C,\\ \xi^+ &\in G(\xi) \quad \xi \in D,\end{aligned}$$

where $\xi \in \mathbb{R}^n$ is the state, $C \subset \mathbb{R}^n$ is the flow set, $F : \mathbb{R}^n \rightrightarrows \mathbb{R}^n$ is the flow map, $D \subset \mathbb{R}^n$ denotes the jump set, and $G : \mathbb{R}^n \rightrightarrows \mathbb{R}^n$ denotes the jump map, where the notation $\rightrightarrows$ indicates that F and G are set-valued maps. A solution ξ to $\mathcal{H}$ is parametrized by (t, j), where t denotes ordinary time and j denotes the jump time, and its domain $\mathrm{dom}\,\xi \subset \mathbb{R}_{\geq 0} \times \mathbb{N}$ is a hybrid time domain: for each $(T, J) \in \mathrm{dom}\,\xi$, $\mathrm{dom}\,\xi \cap ([0, T] \times \{0, 1, \dots J\})$ can be written in the form $\cup_{j=0}^{J-1}([t_j, t_{j+1}], j)$ for some finite sequence of times $0 = t_0 \leq t_1 \leq t_2 \leq \cdots \leq t_J$, where t_j's define the jump times. A solution ξ to a hybrid system is said to be *maximal* if it cannot be extended by flowing nor jumping, and *complete* if its domain is unbounded. The projection of solutions onto the t direction is given by $\xi{\downarrow_t}(t) := \xi(t, J(t))$, where $J(t) := \max\{j : (t, j) \in \mathrm{dom}\,\xi\}$. The distance of a point $\xi \in \mathbb{R}^n$ to a closed set $\mathcal{A} \subset \mathbb{R}^n$ is given by $|\xi|_{\mathcal{A}} := \inf_{y\in\mathcal{A}} |y - \xi|$ and $\mathcal{A}$ is said to be: stable for $\mathcal{H}$ if for every $\epsilon > 0$ there exists $\delta > 0$ such that every solution ξ to $\mathcal{H}$ with $|\xi(0, 0)|_{\mathcal{A}} \leq \delta$ satisfies $|\xi(t, j)|_{\mathcal{A}} \leq \epsilon$ for all $(t, j) \in \mathrm{dom}\,\xi$; globally attractive for $\mathcal{H}$ if each maximal solution ξ is complete and $\lim_{t+j\to\infty} |\xi(t, j)|_{\mathcal{A}} = 0$; globally asymptotically stable for $\mathcal{H}$ if it is both stable and globally attractive for $\mathcal{H}$.

The notion of a smooth manifold is taken from [23] and it is as follows: an n-dimensional smooth manifold is comprised of an n-dimensional topological manifold $\mathscr{M}$ and a maximal smooth atlas $\mathscr{A}$ on $\mathscr{M}$. A maximal smooth atlas $\mathscr{A}$ of $\mathscr{M}$ is a collection of smooth charts $\{(U_i, \psi_i)\}_{i\in\mathcal{N}}$ (indefinitely continuously differentiable) that are smoothly compatible. This means that: U_i are open subsets of $\mathscr{M}$ that cover $\mathscr{M}$, $\psi_i : U_i \to \mathbb{R}^n$ and $\psi_j \circ \psi_i^{-1} : \psi_i(U_j \cap U_i) \to \mathbb{R}^n$ are smooth invertible functions for each $i, j \in \mathcal{N}$, known in the robotics literature as *generalized coordinates* (c.f. [3]).

III. Problem Setup

In this paper, we consider dynamical systems evolving on a compact smooth manifold without boundary, denoted by $\mathscr{M}$, with dimension n and properly embedded in $\mathbb{R}^m$ with $m > n$, described by

$$\begin{aligned}\dot x &= \Pi(x)\omega\\ \dot\omega &= u\end{aligned} \tag{1}$$

where $x \in \mathscr{M}$, $\omega \in \mathbb{R}^k$, $u \in \mathbb{R}^k$ is the input, and $x \mapsto \Pi(x) \in \mathbb{R}^{m\times k}$ is a continuous map whose image at $x \in \mathscr{M}$ is the tangent space to $\mathscr{M}$ at x, denoted by $\mathsf{T}_x\mathscr{M} \subset \mathbb{R}^m$, i.e., the following is satisfied

$$\{y \in \mathbb{R}^m : y = \Pi(x)v \text{ for some } v \in \mathbb{R}^k\} = \mathsf{T}_x\mathscr{M}$$

for each $x \in \mathscr{M}$.

For controller design purposes, we assume that $\mathscr{M}$ is endowed with a smooth structure that satisfies the following assumption.

Assumption 1. *Given a compact smooth manifold without boundary $\mathscr{M}$ with dimension n and $r \in \mathscr{M}$, let $\mathscr{A} := \{(U_i, \psi_i)\}_{i \in \mathscr{N}}$ denote a smooth maximal atlas of $\mathscr{M}$ where $\mathscr{N}$ is a finite discrete topological space and $\psi_i(U_i) = \mathbb{R}^n$ for each $i \in \mathscr{N}$. Then, we assume that $r \in U_i$ for each $i \in \mathscr{N}$.*

In this paper, our goal is to design a hybrid controller

$$\begin{aligned} \dot{q} &\in F_c(x, \omega, q) \quad (x, \omega, q) \in C \subset \Xi \\ q^+ &\in G_c(x, \omega, q) \quad (x, \omega, q) \in D \subset \Xi \end{aligned} \tag{2}$$

with $\Xi := \mathscr{M} \times \mathbb{R}^k \times \mathscr{N}$ and output $u = \kappa(x, \omega, q)$ defined for each $(x, \omega, q) \in C$ such that, for some given $r \in \mathscr{M}$, the set

$$\mathcal{A} := \{(x, \omega, q) \in \Xi : x = r, \omega = 0\} \tag{3}$$

is globally asymptotically stable for the interconnection between (1) and (2). Note that (2) measures (x, ω) which is the state of (1).

IV. Controller Design

For controller design purposes, let V denote a continuously differentiable function from $\mathbb{R}^n$ to $\mathbb{R}_{\geq 0}$ satisfying the following: 1) $\nabla V(y) = 0 \implies y = 0$;[1] 2) there exist $\underline{\alpha}, \overline{\alpha} \in \mathcal{K}_\infty$ such that $\underline{\alpha}(|y|) \leq V(y) \leq \overline{\alpha}(|y|)$ for each $y \in \mathbb{R}^n$.

Under Assumption 1, let

$$\hat{V}(x, q) := \begin{cases} V(\psi_q(x) - \psi_q(r)) & \text{if } (x, q) \in \mathscr{W} \\ +\infty & \text{otherwise} \end{cases},$$

for each $(x, q) \in \mathscr{M} \times \mathscr{N}$, where $\mathscr{W} := \{(x, q) \in \mathscr{M} \times \mathscr{N} : x \in U_q\}$. We devise a hybrid controller as follows:

$$\begin{aligned} \dot{q} &= 0 \qquad (x, \omega, q) \in C := \{(x, \omega, q) \in \Xi : \mu(x, q) \leq \delta\} \\ q^+ &\in \varrho(x) \quad (x, \omega, q) \in D := \{(x, \omega, q) \in \Xi : \mu(x, q) \geq \delta\} \end{aligned} \tag{4}$$

where $\delta > 0$,

$$\mu(x, q) := \hat{V}(x, q) - \nu(x) \tag{5}$$

for each $(x, q) \in \mathscr{M} \times \mathscr{N}$, and

$$\varrho(x) := \arg\min_{p \in \mathscr{N}} \hat{V}(x, p) \qquad \forall x \in \mathscr{M}, \tag{6a}$$

$$\nu(x) := \min_{p \in \mathscr{N}} \hat{V}(x, p) \qquad \forall x \in \mathscr{M}, \tag{6b}$$

with $r \in \mathscr{M}$ satisfying Assumption 1, which guarantees that $\psi_q(r)$ is defined for each $q \in \mathscr{N}$.

Moreover, given $k_\omega > 0$, we define the output of the hybrid controller (4) as the following control law:

$$\kappa(x, \omega, q) := -\Pi(x)^\top \mathcal{D}\psi_q(x)^\top \nabla V\left(\psi_q(x) - \psi_q(r)\right) - k_\omega \omega, \tag{7}$$

for each $(x, q) \in \mathscr{W}$ and $\omega \in \mathbb{R}^k$, where $\nabla V(y)$ denotes the gradient of $y \mapsto V(y)$ evaluated at y.

[1] A function $\alpha : \mathbb{R}_{\geq 0} \to \mathbb{R}_{\geq 0}$ is a class-$\mathcal{K}_\infty$ function, also written $\alpha \in \mathcal{K}_\infty$, if α is zero at zero, continuous, strictly increasing, and unbounded. Given a compact smooth manifold $\mathscr{M}$ and an atlas satisfying Assumption 1, one may conveniently select $V(y) = |y|^2 / 2$ for each $y \in \mathbb{R}^n$.

Using the hybrid controller in (4) with output (7), the closed-loop system resulting from the interconnection between (1) and (4) is given by

$$\begin{aligned} \begin{pmatrix} \dot{x} \\ \dot{\omega} \\ \dot{q} \end{pmatrix} &= F(x, \omega, q) := \begin{pmatrix} \Pi(x)\omega \\ \kappa(x, \omega, q) \\ 0 \end{pmatrix} \quad (x, \omega, q) \in C, \\ \begin{pmatrix} x^+ \\ \omega^+ \\ q^+ \end{pmatrix} &\in G(x, \omega, q) := \begin{pmatrix} x \\ \omega \\ \varrho(x) \end{pmatrix} \qquad (x, \omega, q) \in D. \end{aligned} \tag{8}$$

Under Assumption 1, the closed-loop hybrid system satisfies the hybrid basic conditions [22, Assumption 6.5], which are instrumental in guaranteeing robust stability of compact sets (c.f. [22, Chapter 6]). To prove this, we make use of the following intermediate results, which we provide without proof due to space constraints.

Lemma 1. *Let Assumption 1 hold. Then, the function ϱ, given in* (6a)*, is outer semicontinuous, and the function ν, given in* (6b)*, is continuous and satisfies $\nu(x) < +\infty$ for each $x \in \mathscr{M}$.*

Lemma 2. *Let Assumption 1 hold. Then, the function μ in* (5) *is continuous.*

Finally, we present the main result of this section, which guarantees global asymptotic stabilization of a given reference for the closed-loop hybrid system in (8).

Theorem 1. *Let Assumption 1 hold. Then, the set* (3) *is globally asymptotically stable for the system* (8)*.*

Sketch of proof:. We show that the hybrid system (8) satisfies the hybrid basic conditions. Then, we show that

$$\overline{W}(x, \omega, q) := \hat{V}(x, q) + \frac{1}{2}\omega^\top \omega,$$

is nonincreasing for each solution to (8); thus $\mathcal{A}$ is stable. It follows from [22, Proposition 2.10] that each maximal solution to (8) is complete and from [22, Theorem 8.2] it follows that complete solutions converge to (3); hence $\mathcal{A}$ is globally attractive. □

In the next section, we show how the proposed strategy can be applied to the stabilization of a setpoint in $\mathsf{SO}(3)$.

V. Application to Attitude Stabilization for a Rigid-Body

In this section, we demonstrate the applicability of the controller proposed in Section IV to the stabilization of an attitude reference for a rigid-body, which is governed by the equations of motion

$$\dot{R} = RS(\omega), \tag{9a}$$

$$J\dot{\omega} = S(J\omega)\omega + \tau, \tag{9b}$$

where $R \in \mathsf{SO}(3) := \{R \in \mathbb{R}^{3\times 3} : \det(R) = 1,\ R^\top R = I_3\}$ represents the attitude of the rigid-body, $\omega \in \mathbb{R}^3$ represents its angular velocity, $J \in \mathbb{R}^{3\times 3}$ denotes the tensor

of inertia, $\tau \in \mathbb{R}^3$ is the torque input, and $S : \mathbb{R}^3 \to \mathfrak{so}(3)$ is given by

$$S(\omega) := \begin{bmatrix} 0 & -\omega_3 & \omega_2 \\ \omega_3 & 0 & -\omega_1 \\ -\omega_2 & \omega_1 & 0 \end{bmatrix}$$

for each $\omega := (\omega_1, \omega_2, \omega_3) \in \mathbb{R}^3$ (see e.g. [4, p. 281]), where $\mathfrak{so}(3) := \{X \in \mathbb{R}^{3\times 3} : X = -X^\top\}$ is the Lie Algebra of $\mathsf{SO(3)}$. Noting that $R \in \mathsf{SO(3)}$ can be regarded as an element of $\mathbb{R}^9$ by means of the map $x := \mathrm{vec}(R)$ with inverse $\mathsf{M}_{3,3} : \mathbb{R}^9 \to \mathbb{R}^{3\times 3}$, we have that

$$\dot{x} = -\begin{bmatrix} RS(e_1)\omega \\ RS(e_2)\omega \\ RS(e_3)\omega \end{bmatrix} = -(I_3 \otimes R)\Gamma\omega \tag{10}$$

where $\Gamma := -\begin{bmatrix} S(e_1) & S(e_2) & S(e_3) \end{bmatrix}^\top$. Replacing $R = \mathsf{M}_{3,3}(x)$ into (10) and

$$\tau := Ju - S(J\omega)\omega. \tag{11}$$

into (9b), it is possible to verify that the system (9) can be cast as (1) with

$$\Pi(x) := -(I_3 \otimes \mathsf{M}_{3,3}(x))\Gamma \quad \forall x \in \mathbb{R}^9.$$

In order to demonstrate the controller design of Section IV is suitable for the application at hand, we show that the maximal atlas generated by the *Cayley transform* satisfies Assumption 1.

A. A maximal atlas for $\mathsf{SO(3)}$

The Cayley transform is the map $\mathsf{C} : \mathfrak{so}(3) \to \mathsf{SO(3)}$ given by $\mathsf{C}(X) := (I_3 - X)(I_3 + X)^{-1}$, for each $X \in \mathfrak{so}(3) := \{X \in \mathbb{R}^{3\times 3} : X^\top = -X\}$, with inverse $\mathsf{C}^{-1}(R) := (I_3 + R)^{-1}(I_3 - R)$, for each $R \in U := \{R \in \mathsf{SO(3)} : R + I_3 \text{ is nonsingular}\}$. The set U corresponds to the set of all rotation matrices minus the rotations by $180\,\mathrm{deg}$. To see this, let us introduce the *Rodrigues' rotation formula* [24], given by

$$\begin{aligned} \mathcal{R}(v,\theta) :=& \exp(\theta S(v)) \\ =& I_3 + \sin(\theta)S(v) + (1 - \cos(\theta))S(v)^2 \end{aligned} \tag{12}$$

for each $(v, \theta) \in \mathsf{S}^2 \times [0, \pi]$, where $\mathsf{S}^n := \{x \in \mathbb{R}^{n+1} : x^\top x = 1\}$ with $n \in \mathbb{N}$ denotes the n-dimensional sphere and, since the eigenvalues of a rotation matrix have unitary norm, if $R + I_3$ is singular, then the eigenvalues of R are $\lambda_1 = 1$ and $\lambda_2 = \lambda_3 = -1$, which implies that $\mathrm{tr}(R) = -1$. Using (12), it follows that $\mathrm{tr}(\mathcal{R}(v,\theta)) = -1 \iff \cos\theta = -1$, thus we conclude that $\mathsf{SO(3)}\backslash U := \{R \in \mathbb{R}^{3\times 3} : R = 2vv^\top - I_3 \text{ for some } v \in \mathsf{S}^2\}$. Using the Cayley transform, it is possible to construct a maximal atlas for $\mathsf{SO(3)}$ which satisfies Assumption 1, as shown next.

Proposition 1. *Let* $U_0 := U$,

$$U_q := \{R \in \mathbb{R}^{3\times 3} : \mathcal{R}(e_q, \pi/2)R \in U\}$$

for each $q \in \{1, 2, 3\}$, *and*

$$\begin{aligned} \psi_0(R) &:= S^{-1}(\mathsf{C}^{-1}(R)) && \forall R \in U_0 \\ \psi_q(R) &:= S^{-1}(\mathsf{C}^{-1}(\mathcal{R}(e_q, \pi/2)R)) && \forall R \in U_q \end{aligned}$$

for each $q \in \{1, 2, 3\}$, *then* $\mathscr{A} := \{(U_i, \psi_i)\}_{i\in\mathscr{N}}$ *with* $\mathscr{N} := \{0, 1, 2, 3\}$ *is a maximal atlas for* $\mathsf{SO(3)}$ *and* $\psi_q(U_q) = \mathbb{R}^3$ *for each* $q \in \mathscr{N}$.

Proof. The proof follows closely the one in [25]. □

B. Simulation Results

Using the function $V(y) := |y|^2/2$, defined for each $y \in \mathbb{R}^3$ and the atlas $\mathscr{A} := \{(U_q, \psi_q)\}_{q\in\mathscr{N}}$ given in Proposition 1, which satisfies Assumption 1, we are able to apply the hybrid controller proposed in Section IV. The interconnection between (9) and (4) is given by

$$\begin{aligned} \begin{pmatrix} \dot{R} \\ \dot{\omega} \\ \dot{q} \end{pmatrix} &= F(R,\omega,q) = \begin{pmatrix} RS(\omega) \\ \kappa(R,\omega,q) \\ 0 \end{pmatrix} && (R,\omega,q) \in C, \\ \begin{pmatrix} R^+ \\ \omega^+ \\ q^+ \end{pmatrix} &\in G(R,\omega,q) = \begin{pmatrix} R \\ \omega \\ \varrho(R) \end{pmatrix} && (R,\omega,q) \in D, \end{aligned} \tag{13}$$

where we made use of (11) and assigned the virtual input u in (11) to κ, given by

$$\begin{aligned} \kappa(R,\omega,q) =& -k_\omega\omega \\ & - \Gamma^\top(I_3 \otimes R^\top)\mathcal{D}\psi_q(R)^\top\nabla V(\psi_q(R) - \psi_q(R_d)) \end{aligned}$$

for each (R, ω, q) satisfying $R \in U_q$, $\omega \in \mathbb{R}^3$. For simulation purposes, we select the reference $R_d = I_3$ and we set $\delta = 1$ and $k_\omega = 2$. The initial conditions are

$$\begin{aligned} R(0,0) &\approx \begin{bmatrix} 0.0253 & -0.9994 & 0.0243 \\ -0.9994 & -0.0259 & -0.0237 \\ 0.0243 & -0.0237 & -0.9994 \end{bmatrix}, \\ \omega(0,0) &= \begin{bmatrix} 0 & 0 & 3 \end{bmatrix}^\top, \\ q(0,0) &= 1, \end{aligned} \tag{14}$$

and were purposely selected to lie in the jump set in order to trigger an initial jump, but also to generate a second jump before converging to the origin. Figure 1 portrays the simulation results which were obtained using the Hybrid Equations Toolbox, described in [26], where the first plot presents the evolution of μ as a function of time and shows that there is a jump once $\mu(x{\downarrow_t}(t), q{\downarrow_t}(t))$ is equal to 1, meaning that the attitude of the rigid-body is approaching an unwanted critical point. The jump does does not affect the values of x and ω, and the attitude error and the norm of the angular velocity converge to 0, as shown in the second and third plots, respectively. Note that, at least for some time after the jump, we have μ equal to 0, meaning that the current logic variable yields the minimum value of $W(R,q) := V(\psi_q(R) - \psi_q(R_d))$ for each $(R,q) \in \mathscr{W}$ and $R_d := I_3$.

C. Robustness to Perturbations

Given the atlas $\mathscr{A} := \{(U_i, \psi_i)\}_{i\in\mathscr{N}}$ of $\mathsf{SO(3)}$ constructed in Proposition 1 and a reference $R_d \in \mathsf{SO(3)}$, a key property of the controller design presented in Section IV is $\lim_{R\to\mathsf{SO(3)}\backslash U_q} W(R,q) = +\infty$, where $W(R,q) := V(\psi_q(R) - \psi_q(R_d))$ for each $(R,q) \in \mathscr{W}$. Since $\mathscr{A}$ covers $\mathsf{SO(3)}$, it follows that any continuous path ϕ :

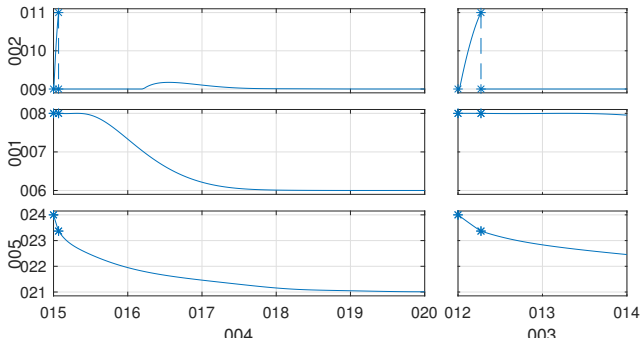

Fig. 1. Evolution of the the functions μ, the attitude error $\mathrm{tr}(I_3 - R^\top R_d)$ and the norm of ω with continuous time for a solution to (8) with initial condition (14).

$\mathbb{R}_{>0} \to \mathsf{SO}(3) \times \mathscr{N}$ converging to $(\mathsf{SO}(3) \times \mathscr{N}) \backslash \mathscr{W}$ satisfies $\mu(R, q) \geq \delta$ for some $t \geq 0$.

In the literature of synergistic potential functions, the function (5) is referred to as the synergy gap, and the parameter δ is the lower bound on the synergy gap that enables controller switching (see, e.g., [16]). Even though the controller design in Section IV resembles synergistic hybrid feedback, it is different in the sense that the synergy gap can be set to an arbitrarily large value, thus improving the robustness of the closed-loop system to exogenous perturbations at the cost of increased input demand.

To illustrate how the behavior of the closed-loop system is affected by the presence of input disturbances and how one may use the parameter δ to mitigate its adverse effects, consider the following perturbed hybrid system:

$$\begin{aligned} \begin{pmatrix} \dot{\hat{R}} \\ \dot{\hat{\omega}} \\ \dot{\hat{q}} \end{pmatrix} &:= \begin{pmatrix} \hat{R}S(\hat{\omega}) \\ \kappa(\hat{R}, \hat{\omega}, \hat{q}) + \epsilon(\hat{R}) \\ 0 \end{pmatrix} && (\hat{R}, \hat{\omega}, \hat{q}) \in \hat{C}, \\ \begin{pmatrix} \hat{R}^+ \\ \hat{\omega}^+ \\ \hat{q}^+ \end{pmatrix} &\in \begin{pmatrix} \hat{R} \\ \hat{\omega} \\ \varrho(\hat{R}) \end{pmatrix} && (\hat{R}, \hat{\omega}, \hat{q}) \in \hat{D}, \end{aligned} \tag{15}$$

where

$$\begin{aligned} \hat{C} &:= \{(\hat{R}, \hat{\omega}, \hat{q}) \in \mathsf{SO}(3) \times \mathbb{R}^3 \times \mathscr{N} : \mu(\hat{R}, \hat{q}) \leq \hat{\delta}\}, \\ \hat{D} &:= \{(\hat{R}, \hat{\omega}, \hat{q}) \in \mathsf{SO}(3) \times \mathbb{R}^3 \times \mathscr{N} : \mu(\hat{R}, \hat{q}) \geq \hat{\delta}\}. \end{aligned}$$

and, for each $\hat{R} \in U_{\hat{q}}$,

$$\epsilon(\hat{R}) = -(1+\bar{\epsilon})\Gamma^\top (I_3 \otimes \hat{R}^\top) \mathcal{D}\psi_{\hat{q}}(\hat{R})^\top \nabla V(\psi_{\hat{q}}(\hat{R}) - \psi_{\hat{q}}(R_d))$$

with $\bar{\epsilon} > 0$ is an exogenous disturbance that counteracts the effect of the proportional term of the control law κ, thus preventing the stabilization of the desired reference. Figure 2 presents the simulation results for the hybrid system which combines the dynamics of (13) and (15), with (13) affected by the perturbation $\hat{R} \mapsto \epsilon(\hat{R})$ generated by (15), that is, the hybrid system described by

$$\begin{aligned} \dot{\xi} &= \begin{pmatrix} RS(\omega) \\ \kappa(R, \omega, q) + \epsilon(\hat{R}) \\ 0 \\ \hat{R}S(\hat{\omega}) \\ \kappa(\hat{R}, \hat{\omega}, \hat{q}) + \epsilon(\hat{R}) \\ 0 \end{pmatrix} && \xi \in C \times \hat{C} \\ \xi^+ &\in G_1(\xi) \cup G_2(\xi) && \xi \in D_1 \cup D_2 \end{aligned} \tag{16}$$

where $\xi := (R, \omega, q, \hat{R}, \hat{\omega}, \hat{q})$ and

$$G_1(\xi) := \begin{cases} G(R, \omega, q) \times \{(\hat{R}, \hat{\omega}, \hat{q})\} \\ \quad \text{if } \xi \in D_1 := D \times \mathsf{SO}(3) \times \mathbb{R}^3 \times \mathscr{N} \\ \emptyset \text{ otherwise} \end{cases}, \tag{17a}$$

$$G_2(\xi) := \begin{cases} \{(R, \omega, q)\} \times G(\hat{R}, \hat{\omega}, \hat{q}) \\ \quad \text{if } \xi \in D_2 := \mathsf{SO}(3) \times \mathbb{R}^3 \times \mathscr{N} \times \hat{D} \\ \emptyset \text{ otherwise} \end{cases}. \tag{17b}$$

In these simulations, we use the same controller parameters for both closed-loop systems, except for $\hat{\delta}$ which is set to 0.01, and the initial conditions are

$$\begin{aligned} R(0,0) = \hat{R}(0,0) &\approx \begin{bmatrix} 1.0000 & 0 & 0 \\ 0 & -0.8012 & -0.5984 \\ 0 & 0.5984 & -0.8012 \end{bmatrix}, \\ \hat{\omega}(0,0) &\approx \begin{bmatrix} 0.0776 & 0 & 0 \end{bmatrix}^\top, \ \omega(0,0) \approx \begin{bmatrix} 0.8571 & 0 & 0 \end{bmatrix}^\top, \\ q(0,0) &= \hat{q}(0,0) = 2. \end{aligned} \tag{18}$$

The analysis of Figure 2 reveals that $t \mapsto R{\downarrow_t}(t)$ is converging to a neighborhood of the desired equilibrium point while $t \mapsto \hat{R}{\downarrow_t}(t)$ remains at a distance. We conclude that the closed-loop system with the higher synergy gap is able to overcome the disturbances ϵ and converge to a neighborhood of the equilibrium point. It should be pointed out that, similarly to (16), it is possible to craft a disturbance that prevents the asymptotic stabilization of the nominal system (R, ω, q). However, doing so also prevents the asymptotic stabilization of $(\hat{R}, \hat{\omega}, \hat{q})$, as shown in Figure 3.

Figure 3 represents the evolution with time of a solution to

$$\begin{aligned} \dot{\xi} &= \begin{pmatrix} RS(\omega) \\ \kappa(R, \omega, q) + \epsilon(R) \\ 0 \\ \hat{R}S(\hat{\omega}) \\ \kappa(\hat{R}, \hat{\omega}, \hat{q}) + \epsilon(R) \\ 0 \end{pmatrix} && \xi \in C \times \hat{C} \\ \xi^+ &\in G_1(\xi) \cup G_2(\xi) && \xi \in D_1 \cup D_2 \end{aligned} \tag{19}$$

for the initial condition (18). It is possible to verify that, even though the disturbance $R \to \epsilon(R)$ was constructed to prevent the stabilization of (R, ω, q), it also prevents the stabilization of $(\hat{R}, \hat{\omega}, \hat{q})$.

Finally, note that controller switching usually leads to control inputs that are discontinuous, and this may be an

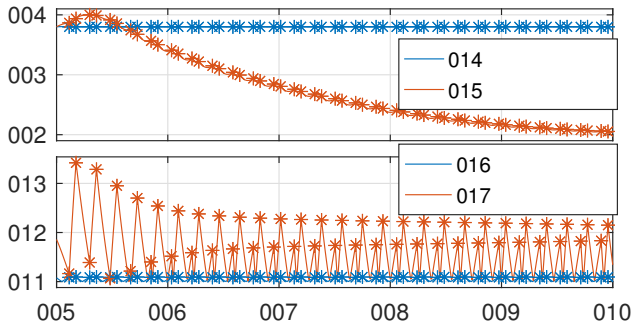

Fig. 2. Simulation results for the hybrid system (16) with initial condition (18).

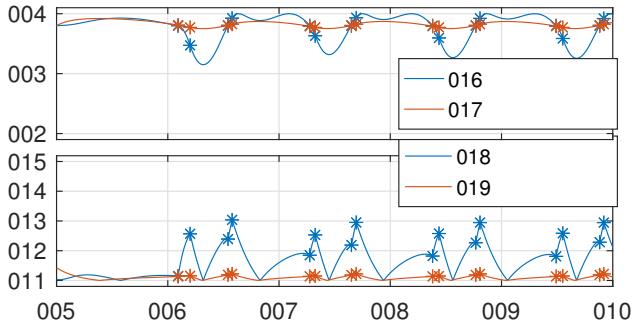

Fig. 3. Simulation results for the hybrid system (19) with initial condition (18).

unreasonable assumption for some applications. Further research efforts will focus on the smoothing of the control input.

VI. Conclusions

In this paper, we presented a controller for global asymptotic stabilization of a setpoint on a manifold that draws inspiration from existing control strategies based on synergistic potential functions. Given a function that is continuously differentiable and positive definite, we used local coordinate charts to design a controller that stabilizes the setpoint through gradient-based feedback during flows, and jumps to a lower value near unwanted critical points.

We evaluated the proposed strategy through the problem of stabilizing a given attitude reference for a rigid-body vehicle. Key concepts of synergistic potential functions, such as the synergy gap, are illustrated for this system, and the behavior of the closed-loop system is tested by means of simulations.

References

[1] A. M. Lyapunov, *The general problem of the stability of motion*. Taylor & Francis, 1992.

[2] H. K. Khalil, *Nonlinear systems*. Prentice Hall, 2002.

[3] A. M. Bloch, *Nonholonomic Mechanics and Control*, vol. 24 of *Interdisciplinary Applied Mathematics*. New York: Springer, 2003.

[4] F. Bullo and A. D. Lewis, *Geometric control of mechanical systems: modeling, analysis, and design for simple mechanical control systems*. Springer, 2005.

[5] D. H. S. Maithripala, J. M. Berg, and W. P. Dayawansa, "Almost-global tracking of simple mechanical systems on a general class of Lie groups," *IEEE Transactions on Automatic Control*, vol. 51, no. 2, pp. 216–225, 2006.

[6] S. P. Bhat and D. S. Bernstein, "A topological obstruction to continuous global stabilization of rotational motion and the unwinding phenomenon," *Systems & Control Letters*, vol. 39, no. 1, pp. 63–70, 2000.

[7] M. Malisoff, M. Krichman, and E. Sontag, "Global Stabilization for Systems Evolving on Manifolds," *Journal of Dynamical and Control Systems*, vol. 12, no. 2, pp. 161–184, 2006.

[8] O.-E. Fjellstad and T. Fossen, "Singularity-free tracking of unmanned underwater vehicles in 6 DOF," in *Proceedings of the 33rd IEEE Conference on Decision and Control*, vol. 2, pp. 1128–1133, IEEE, 1994.

[9] C. G. Mayhew and A. R. Teel, "On the topological structure of attraction basins for differential inclusions," *Systems & Control Letters*, vol. 60, no. 12, pp. 1045–1050, 2011.

[10] C. G. Mayhew, R. G. Sanfelice, and A. R. Teel, "Synergistic Lyapunov functions and backstepping hybrid feedbacks," in *Proceedings of the 2011 American Control Conference*, pp. 3203–3208, IEEE, jun 2011.

[11] C. G. Mayhew, R. G. Sanfelice, and A. R. Teel, "Further results on synergistic Lyapunov functions and hybrid feedback design through backstepping," in *Proceedings of the 50th IEEE Conference on Decision and Control and European Control Conference*, pp. 7428–7433, IEEE, 2011.

[12] R. Sanfelice, M. Messina, S. Emre Tuna, and A. Teel, "Robust hybrid controllers for continuous-time systems with applications to obstacle avoidance and regulation to disconnected set of points," in *Proceedings of the 2006 American Control Conference*, 2006.

[13] R. G. Sanfelice, A. R. Teel, and R. Goebel, "Supervising a Family of Hybrid Controllers for Robust Global Asymptotic Stabilization," in *Proceedings of the 47th Conference on Decision and Control*, pp. 4700–4705, 2008.

[14] C. G. Mayhew and A. R. Teel, "Hybrid control of spherical orientation," in *Proceedings of the 49th IEEE Conference on Decision and Control*, pp. 4198–4203, IEEE, 2010.

[15] C. G. Mayhew, R. G. Sanfelice, and A. R. Teel, "Quaternion-Based Hybrid Control for Robust Global Attitude Tracking," *IEEE Transactions on Automatic Control*, vol. 56, no. 11, pp. 2555–2566, 2011.

[16] C. G. Mayhew and A. R. Teel, "Synergistic Hybrid Feedback for Global Rigid-Body Attitude Tracking on SO(3)," *IEEE Transactions on Automatic Control*, vol. 58, no. 11, pp. 2730–2742, 2013.

[17] S. Berkane, A. Abdessameud, and A. Tayebi, "Global Exponential Stabilization on SO(3) via Hybrid Feedback," *arXiv*, 2015.

[18] T. Lee, "Global Exponential Attitude Tracking Controls on SO(3)," *IEEE Transactions on Automatic Control*, vol. 60, no. 10, pp. 2837–2842, 2015.

[19] S. Berkane and A. Tayebi, "Construction of Synergistic Potential Functions on SO(3) with Application to Velocity-Free Hybrid Attitude Stabilization," *IEEE Transactions on Automatic Control*, vol. 62, no. 1, 2017.

[20] J.-Y. Wen and K. Kreutz-Delgado, "The attitude control problem," *IEEE Transactions on Automatic Control*, vol. 36, no. 10, pp. 1148–1162, 1991.

[21] P. Casau, C. G. Mayhew, R. G. Sanfelice, and C. Silvestre, "Global exponential stabilization on the n-dimensional sphere," in *Proceedings of the 2015 American Control Conference (ACC)*, pp. 3218–3223, 2015.

[22] R. Goebel, R. G. Sanfelice, and A. R. Teel, *Hybrid Dynamical Systems Modeling, Stability, and Robustness*. Princeton University Press, 2012.

[23] J. M. Lee, *Introduction to Smooth Manifolds*, vol. 218 of *Graduate Texts in Mathematics*. New York: Springer, 2012.

[24] O. Rodrigues, "Des lois géométriques qui régissent les déplacements d'un système solide dans l'espace, et de la variation des coordonnées provenant de ces déplacements considérés indépendamment des causes qui peuvent les produire," *Journal de mathématiques pures et appliquées*, vol. 1, no. 5, pp. 380–440, 1840.

[25] E. W. Grafarend and W. Kühnel, "A minimal atlas for the rotation group SO(3)," *International Journal on Geomathematics*, vol. 2, no. 1, pp. 113–122, 2011.

[26] R. G. Sanfelice, D. Copp, and P. Nanez, "A toolbox for simulation of hybrid systems in Matlab/Simulink: Hybrid Equations (HyEQ) Toolbox," in *Proceedings of the 16th international conference on Hybrid systems: computation and control*, (New York), p. 101, ACM Press, 2013.